**Auxiliary material for Paper 2009GL039496**

# Slip distribution from the 1 April 2007 Solomon Islands earthquake: A unique image of near-trench rupture

**Ting Chen**
School of Earth and Atmospheric Sciences, Georgia Institute of Technology, Atlanta, Georgia, USA and School of Geodesy and Geomatics, Wuhan University, Wuhan, China

**Andrew V. Newman and Lujia Feng**
School of Earth and Atmospheric Sciences, Georgia Institute of Technology, Atlanta, Georgia, USA

**Hermann M. Fritz**
School of Civil and Environmental Engineering, Georgia Institute of Technology, Savannah, Georgia, USA

Chen, T., A. V. Newman, L. Feng, and H. M. Fritz (2009), Slip distribution from the 1 April 2007 Solomon Islands earthquake: A unique image of near-trench rupture, Geophys. Res. Lett., 36, L16307, doi:10.1029/2009GL039496.

## Introduction

The supplementary figures include modeling results that compare and contrast the optimal and alternate dipping solutions at 29 and 20°, respectively (Figure S1); testing of model sensitivity and resolution to alternating boxes with unit slip, or "checkerboard" tests (Figure S2); geospatial mapping of the resolution testing results (Figure S3); and comparative best-estimate results for models that incorporate data from independent, and combined surveys (Figure S4).

## 1. 2009gl039496-fs01.eps

***Figure S1:*** Optimally smoothed solutions at (a) 20° and (b) 29° dip, ($\delta$) are shown. Increased fault width comes from maintaining a lower depth constraint of 40 km over a range of dip angles. (c and d) The trade-off between roughness and RMS misfit is shown for each model. Optimal smoothing is chosen slightly higher for dip, $\delta$=20°: $\kappa$=1100. Solutions remain similar between the two models, with strong shallow slip patches on either side of Simbo Ridge (120 km along-strike). A significant discrepancy between the two dip solutions is the amount of slip bridging the larger slip patches near the surface (around 110-115 km along-strike). 29° dip solution is the preferred model in this study (Fig. 2a).

**2. 2009gl039496-fs02.eps**

***Figure S2:*** "Checkerboard" resolution testing of 29° dip model. The left column (a-c) shows a series of theoretical input slip distributions (black patch with 1 m thrust and white 0 m) using the same geometry as the rupture plane. Forward calculations determine synthetic surface uplifts at our observation points (Figures 1b and 1c). These synthetic data are then inverted to solve for dip-slip at low smoothing ($\kappa$=1). A low smoothing value is chosen in order to determine the resolvability of rapid changes. (d-f) Inverted solutions show the ability of the model and data to resolve thrust on the interface. Input models range from constant [a] 10x10 km blocks, to models that increase blocks with depth, where Figure S2c has reduced 5x5 km block near the surface, and is inverted with 4 times the elements. All models show no resolvability beyond about 160 km along-strike. While the constant 10x10 block model shows good resolvability on the left (east side of fault), the larger blocks are better-resolved down-dip. Solution e is repeated in Figure S3.

**3. 2009gl039496-fs03.eps**

***Figure S3*:** Checkerboard resolution test (Figure S3e) shown in map-view of region. Resolution is most diminished (hashed regions) where model patches are furthest from land (available observation points). Hashed regions are repeated in main-text Figure 3.

**4. 2009gl039496-fs04.eps**

***Figure S4***: Optimal solutions are shown for the combined and independent survey results. The preferred models for each (a) Taylor-only data, (b) Fritz-only data, and combined, (c) Taylor and Fritz data (optimal model in main text Figures 2a and 3). Solutions are for the independent best dip, and optimally chosen smoothing. Also shown are the associated resolution tests (d-f) using the input model in Figure S2c. Overall, the independent data results agree with each other and the combined, but at different dips, and lower resolution. Differences are largely in regions with little or no resolution.

Figure S1.

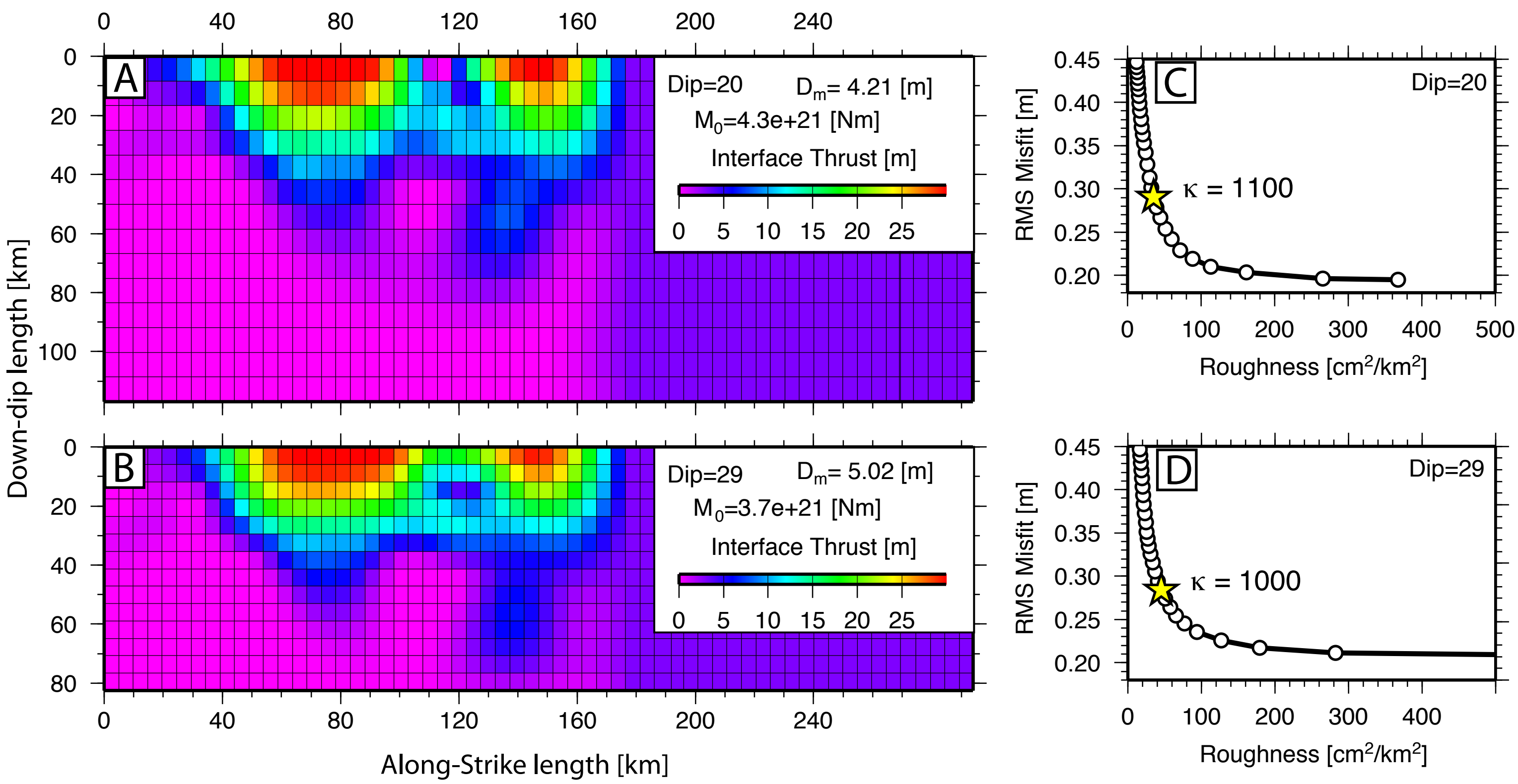
A
Dip=20
$D_m$= 4.21 [m]
$M_0$=4.3e+21 [Nm]
Interface Thrust [m]
0 5 10 15 20 25
B
Dip=29
$D_m$= 5.02 [m]
$M_0$=3.7e+21 [Nm]
Interface Thrust [m]
0 5 10 15 20 25
Down-dip length [km]
Along-Strike length [km]
C
Dip=20
κ = 1100
D
Dip=29
κ = 1000
RMS Misfit [m]
Roughness [cm²/km²]

Figure S2.

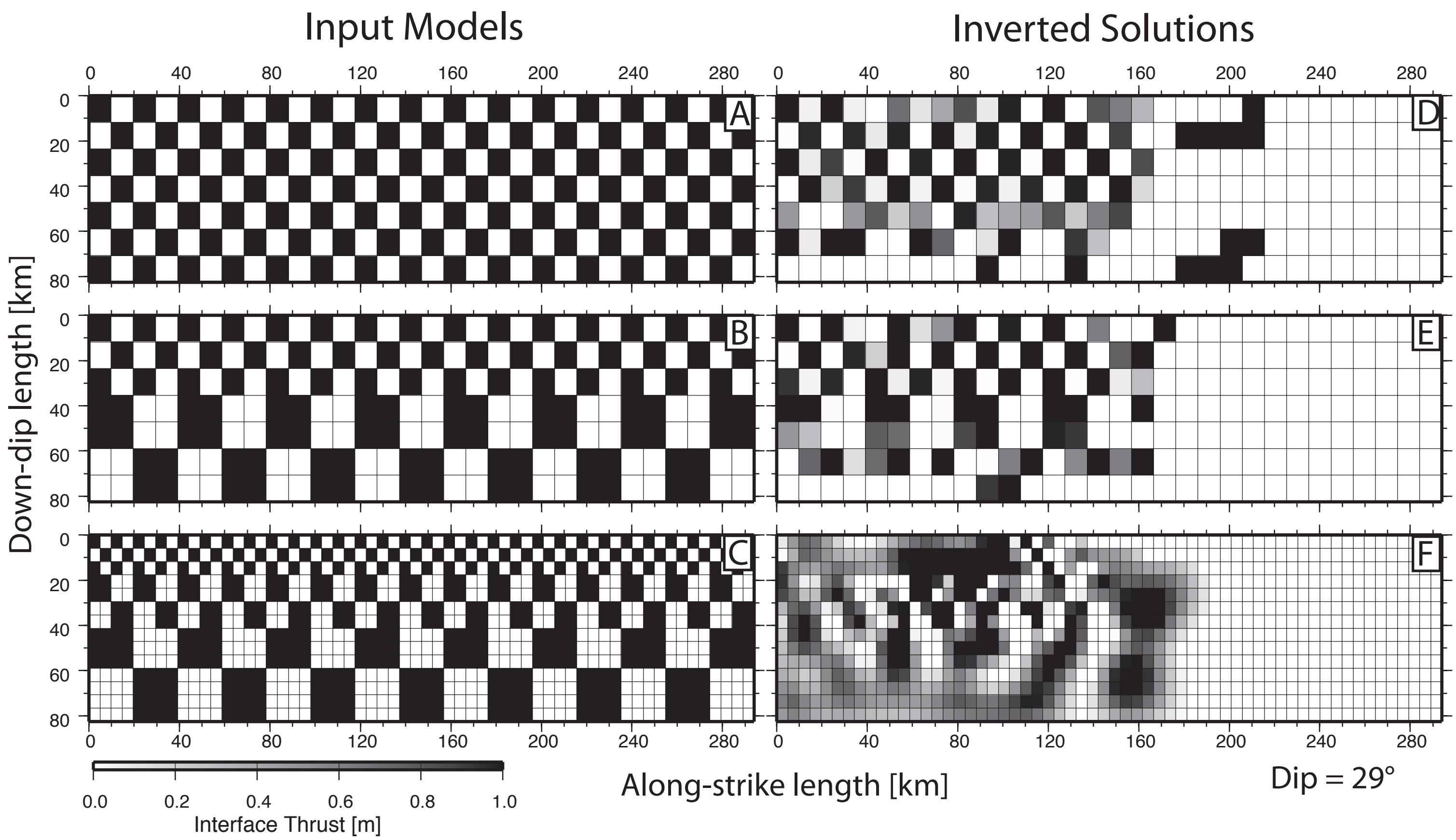

Input Models
Inverted Solutions
A
B
C
D
E
F
0
40
80
120
160
200
240
280
0
20
40
60
80
Down-dip length [km]
Along-strike length [km]
Dip = 29°
0.0
0.2
0.4
0.6
0.8
1.0
Interface Thrust [m]

Figure S3.

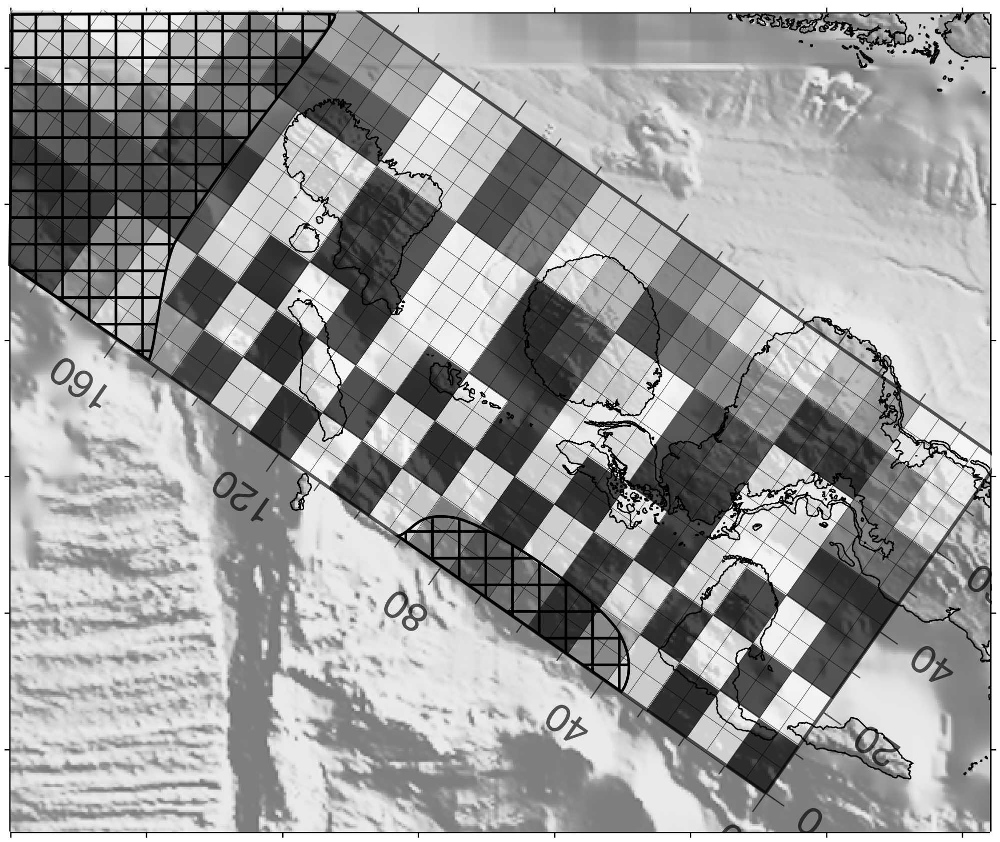

Figure S4.

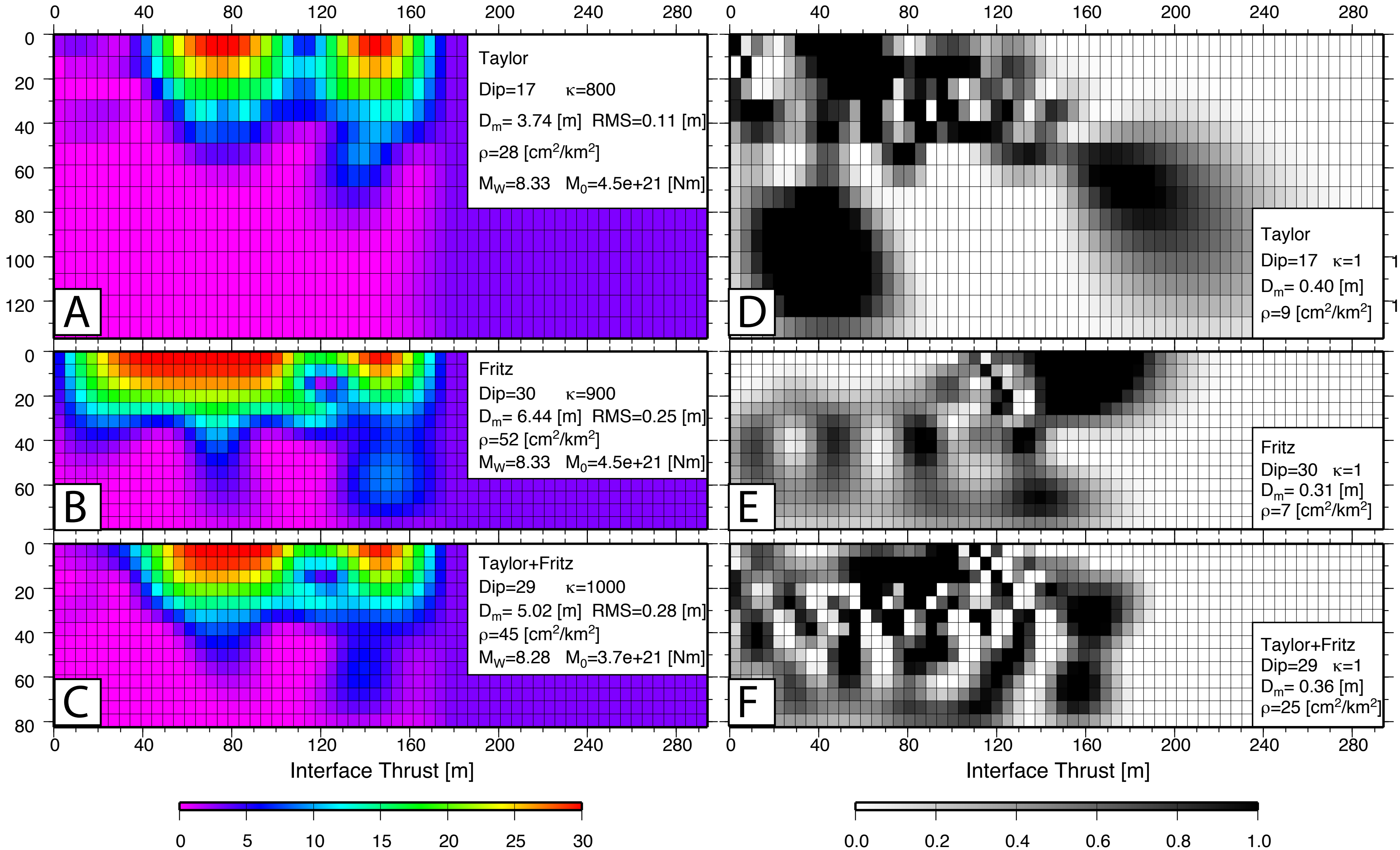

Taylor
Dip=17 κ=800
Dm= 3.74 [m] RMS=0.11 [m]
ρ=28 [cm2/km2]
MW=8.33 M0=4.5e+21 [Nm]
A
Fritz
Dip=30 κ=900
Dm= 6.44 [m] RMS=0.25 [m]
ρ=52 [cm2/km2]
MW=8.33 M0=4.5e+21 [Nm]
B
Taylor+Fritz
Dip=29 κ=1000
Dm= 5.02 [m] RMS=0.28 [m]
ρ=45 [cm2/km2]
MW=8.28 M0=3.7e+21 [Nm]
C
Taylor
Dip=17 κ=1
Dm= 0.40 [m]
ρ=9 [cm2/km2]
D
Fritz
Dip=30 κ=1
Dm= 0.31 [m]
ρ=7 [cm2/km2]
E
Taylor+Fritz
Dip=29 κ=1
Dm= 0.36 [m]
ρ=25 [cm2/km2]
F
Interface Thrust [m]
Interface Thrust [m]
0 5 10 15 20 25 30
0.0 0.2 0.4 0.6 0.8 1.0